1993

# Dipole-dipole spin relaxation in solids. The unrestricted hopping model and the methyl proton - non-methyl proton interaction

Christopher Palmer

Alfonso M. Albano

Peter A. Beckmann
*Bryn Mawr College*, pbeckman@brynmawr.edu

**PHYSICA** B

# Dipole–dipole spin relaxation in solids

The unrestricted hopping model and the methyl proton–non-methyl proton interaction*

Christopher Palmer[1], Alfonso M. Albano and Peter A. Beckmann

*Department of Physics, Bryn Mawr College, Bryn Mawr, PA, USA*

Received 28 September 1992

We develop a stochastic model for molecular reorientation which leads to the calculation of the dipole–dipole spin-lattice relaxation rate in cases where the *length* of the spin–spin vector changes with time. The calculations are applied to methyl group rotation-induced relaxation in planar methyl-substituted aromatic molecules like methylnaphthalenes, methylanthracenes and methylphenanthrenes. Our theory considers an *unrestricted hopping model* in which the spin–spin vector hops from one position to any of its other allowed positions. A general discussion of the relaxation process is presented and a variety of general geometries for the motion of pairs of spins is considered. The case of a reorienting methyl group is considered in some detail. The relaxation rate resulting from the interaction between methyl protons and *any* other fixed proton is then presented. The general approach is appropriate for a large class of molecular solids. We compare previously determined experimental relaxation rates with the current theory for methyl-substituted naphthalenes, anthracenes and phenanthrenes. We show that the geometry for peri-substituted methyl groups corresponds to the situation where the two methyl protons near the peri hydrogen lie out of the plane of the aromatic ring. This expected result is in agreement with laser jet spectroscopy experiments and ab initio calculations for 1-methylnaphthalene.

## 1. Introduction

Nuclear spin relaxation is a very useful technique for the study of molecular dynamics. For an excited nuclear spin system, a spin–space interaction is modulated by motion and the spin system relaxes via stimulated emission by sampling the local time-dependent magnetic field. The interaction of interest in this study is the spin–spin dipolar interaction which dominates the relaxation process for protons in solids. Other spin–space interactions important for the general nuclear spin relaxation problem are re-

viewed elsewhere [1]. The fundamental problem of an ensemble of reorienting isolated spin pairs in contact with a heat bath has been set up in a general manner [2,3]. When particular classes of systems are considered, most theoretical investigations consider the case where the distance between spins is constant and only the orientation of the spin–spin vector with respect to the applied magnetic field is changing. Very limited work has been done for the case where the distance between spins (as well as their relative orientation) changes with time. This latter problem is more complicated and we have investigated it in some detail.

In most organic Van der Waals crystalline and glassy solids, random translational motion is absent on the nuclear magnetic resonance time scale and molecular and intramolecular reorientation can be isolated and studied by the solid state nuclear spin relaxation technique. These latter motions are usually not isotropic and the

*Correspondence to:* P.A. Beckmann, Department of Physics, Bryn Mawr College, Bryn Mawr, PA 19010, USA.

[1] Present address: Analytical Products Division, Milton Roy Company, 820 Linden Avenue, Rochester, NY 14625, USA.

* Part of this work forms part of a dissertation submitted to Bryn Mawr College by CP in partial fulfilment of the requirement of the PhD.

spin–spin vectors are geometrically restricted. In this study, we model the motion by instantaneous hopping among sites. This approach lends itself to a quantum description of dynamical processes.

In order to make these matters more concrete, we show a model molecule, 1-methylnaphthalene ($C_{10}H_7CH_3$), in fig. 1. The methyl ($CH_3$) group reorients about the methyl carbon–ring carbon bond which defines the $z$-axis $z_{MFF}$ of a molecular-fixed reference frame MFF. The spin–spin vector labelled $r^{methyl}$ in fig. 1 takes on three values in the $x_{MFF}$–$y_{MFF}$ plane as the methyl group reorients in its three-fold potential. The vector $r^{methyl}$ is of constant length: only its orientation changes. The nuclear spin relaxation rate resulting from the modulation of this vector is well understood [4,5] and in this paper we will fold the well-known solution to this problem into
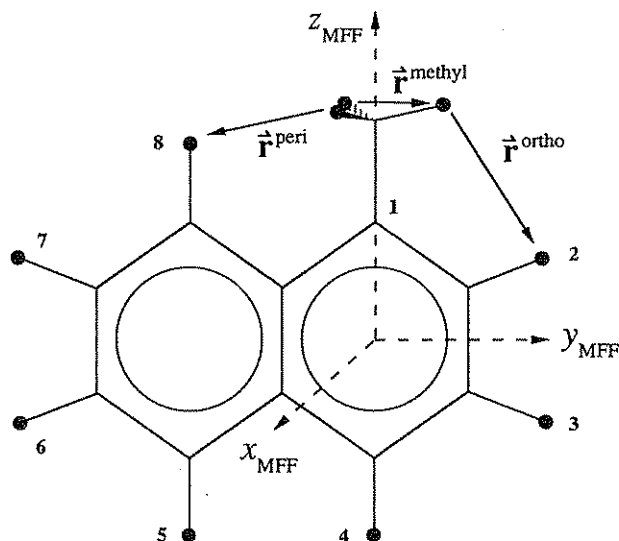
our more general formalism as an introductory example.

Two methyl–nonmethyl spin–spin interactions are shown in 1-methylnaphthalene in fig. 1. Each of the three methyl protons interacts with the neighboring ring peri proton. As the methyl group reorients, the vector $r^{peri}$ between a *single* methyl proton and the peri ring proton takes on three values, one of which is shown in fig. 1. The same is true for the interaction between a *single* methyl proton and the neighboring ring ortho proton. One of three possible values of $r^{ortho}$ for each of the three protons is shown in fig. 1. We emphasize at this early stage that there are three possible values of these vectors because a *single* methyl proton has three positions available to it, not because there are three protons in a methyl group. As the methyl group reorients, these vectors are modulated but the three possible values of $|r^{ortho}|$ and $|r^{peri}|$ for each proton are, in general, different, assuming an arbitrary orientation of the methyl group. (In the methyl position shown in fig. 1, two of the three distances are equal for both these vectors.) The nuclear spin-lattice relaxation rate for this process has not been developed before and we shall do so here.

For all three spin–spin vectors shown in fig. 1, each of the other two possible positions for the vector is accessible in the next jump. That is, the methyl group can hop by $2\pi/3$ either way (or not hop at all). We call this the *unrestricted hopping model* where the vector $r$ can hop from its present position to *any* of the allowed positions.

In the next section we review the fundamental aspects of nuclear spin relaxation in Van der Waals molecular solids, including the individual elements that go into the general assumption of exponential relaxation. In section 3 we develop the general features for stochastic models appropriate for molecular reorientation and in section 4 we develop mathematically the *unrestricted hopping model*. We apply this model to three general geometries in section 4 and apply the most complex of these, the oblique cone geometry, to methyl proton–non-methyl proton interactions in section 5. We then apply these specific geometries to methyl-substituted planar aromatic



Fig. 1. The molecule 1-methylnaphthalene. The molecular fixed frame MFF is characterized by $x_{MFF}$, $y_{MFF}$, $z_{MFF}$. The intramethyl spin–spin vector $r^{methyl}$ reorients in the $x$–$y$ plane as the methyl group reorients. The length $|r^{methyl}|$ is constant. The methyl-ring spin–spin vectors $r^{ortho}$ and $r^{peri}$ are not of constant length for a given methyl proton as a consequence of methyl group reorientation. For the methyl group orientation shown, $\beta = 0$ for the methyl-ortho interaction and $\beta = 60°$ for the methyl-peri interaction. The methyl proton at the end of the solid wedge is above the plane of the page and the methyl proton at the end of the dashed wedge is below the plane of the page. All other atoms are in the plane of the page.

molecules in section 6. The paper is summarized in section 7. We note that much of the algebra in sections 4–6 has been done using *Mathematica*, a software package which combines algebraic manipulation, computational analysis and graphical presentation in very useful ways.

## 2. The relaxation rate $R$

### 2.1. General theory review

The reader is referred to Abragam [2] and Slichter [3] for a review of nuclear magnetic resonance and to our review [1] for a brief discussion of the solid state spin relaxation process. A spin-1/2 particle, in this case a proton (hydrogen nucleus), in a static magnetic field $B$ has two levels separated by an energy $E = \gamma \hbar B = \hbar \omega$ which defines the Larmor angular frequency $\omega$. The parameter $\gamma$ is the magnetogyric ratio of the nucleus. In a solid state proton spin relaxation experiment, the Boltzmann distribution of the populations of the spin system is perturbed by a radio frequency field at frequency $\omega$. The spin system then attempts to return to equilibrium with the other degrees of freedom (the 'lattice'). At the radio wavelengths relevant here, this return to equilibrium occurs only via *stimulated* emission so the spins need to find Larmor frequency (radio) photons in their local environment. These time-dependent magnetic fields (photons) arise if nearby spins are moving. The excited spin system will relax by sampling the Larmor Fourier component of the local fields which themselves reflect the local molecular or intramolecular dynamics.

The hamiltonian for the dipolar interaction between like spins $I_1$ and $I_2$ [6,7] is

$$\mathcal{H} = \left(\frac{24\pi}{5}\right)^{1/2}\left(\frac{\gamma^2\hbar^2}{r^3}\right)\left(\frac{\mu_0}{4\pi}\right)$$
$$\times \sum_{\mu=-2}^{+2} (-1)^\mu Y_{2,-\mu}(\Omega) T_{2,\mu}(I^{(1)}, I^{(2)}) \tag{2.1}$$

where $r = (r, \Omega)$ with $\Omega = \theta^{\mathrm{L}}, \phi^{\mathrm{L}}$ specifies the spin–spin vector in a laboratory fixed frame

(LFF) whose $z$-axis is defined by the applied magnetic field $B$. The superscript L refers to LFF. $Y_{2\mu}$ is the $\mu$th component of a spherical harmonic of order 2. The second-rank spin tensor in eq. (2.1) is defined by Rose [8] in terms of the spherical vectors $I^{(1)}$ and $I^{(2)}$:

$$T_{2,\mu}(I^{(1)}, I^{(2)}) = \sum_{\nu=-1}^{+1} C(1,1,2; \nu, \mu-\nu) I_\nu^{(1)} I_{\mu-\nu}^{(2)} \tag{2.2}$$

where $C(l_1, l_2, l; m_1, m - m_1)$ is a Clebsch–Gordan coefficient [8] and $I_\eta^{(k)}$ is the $\eta$th component of the spherical vector operator for spin $k$ [8]. Since eq. (2.1) is specified in a frame containing the spin quantization axis (i.e. LFF), determining the appropriate spin matrix elements is straightforward [9].

The spin–spin vector $r$ is time dependent due to the molecular motion; this modulates the hamiltonian in eq. (2.1) and causes transitions between the spin states. A perturbed nuclear magnetization

$$\langle \mathcal{M} \rangle = \gamma \hbar \langle I_z \rangle , \tag{2.3}$$

where $\langle \cdot \rangle$ refers to the expectation value, will return to equilibrium via stimulated emission. The appropriate quantum mechanical calculation is done clearly by Abragam [2]. The difference $\Delta \mathcal{M}$ between the instantaneous and equilibrium magnetizations,

$$\Delta \mathcal{M}(t) = \langle \mathcal{M}(t) - \mathcal{M}(\infty) \rangle , \tag{2.4}$$

relaxes exponentially:

$$\Delta \mathcal{M}(t) = \Delta \mathcal{M}(0)\, e^{-Rt} , \tag{2.5}$$

for an ensemble of identical spin pairs that are isolated from each other but in contact with a heat bath.

The spin-lattice relaxation rate $R$ is given [2,3] by

$$R = \frac{3}{2}\left(\frac{\mu_0}{4\pi}\right)^2 \gamma^4\hbar^2 I(I+1)\{J_1(\omega) + 4J_2(2\omega)\} . \tag{2.6}$$

The dipolar hamiltonian in eq. (2.1) is quadratic in the nuclear spin operators, so in order to relax, the spin system picks out the $\omega$ (single spin flip) and the $2\omega$ (double spin flip) components of this local field. At this point we can be more general and express the spectral density $J_{\mu\nu}$ (where $J_\mu$ in eq. (2.6) corresponds to $J_\mu \equiv J_{\mu\mu}$) in terms of the cross correlation function:

$$J_{\mu\nu}(\omega) = \int_{-\infty}^{+\infty} \langle F_\mu^*(0) F_\nu(t) \rangle\, e^{-i\omega t}\, dt,$$  (2.7)

with $F_\mu$ given by

$$F_\mu[r(t)] = \left(\frac{8\pi}{15}\right)^{1/2} \{r(t)\}^{-3} Y_{2\mu}[\Omega(t)].$$  (2.8)

The $Y_{2\mu}$ in eq. (2.8) comes directly from the hamiltonian in eq. (2.1). The correlation function $\langle F_\mu^*(0) F_\nu(t) \rangle$ is discussed further below. The use of $\langle \cdot \rangle$ in eq. (2.7) to mean ensemble average is different from that in eqs. (2.3) and (2.4) where it means quantum mechanical expectation value.

## 2.2. The assumptions

The goal of this work is to develop $R$ from eq. (2.6) in realistic cases where the spin–spin separation $|r|$ varies with time. Little progress has been made on this important problem. There are several important approximations leading to eq. (2.6). It is important to understand these assumptions to see how the limitations affect the way in which our theoretical results can be applied to experimental results. There are three effects being neglected. All three lead to nonexponential relaxation and all three are related.

The first assumption is that spin symmetry effects can be neglected. We assume that if spins are strongly coupled then the observed $R$ can be determined by computing an average $R$ obtained by considering only the mutual pairwise interactions. With this assumption, $R$ for a collection of $M$ spins is given [10] by

$$R = \frac{1}{M} \sum_{\substack{i=1 \\ j \neq i}}^{M} \sum_{j=1}^{M} R_{ij}$$  (2.9)

where $i$, $j$ count the $M$ spins and where each term $R_{ij}$ is given by $R$ in eq. (2.6) with subscripts $i$, $j$ in all the appropriate places in the above equations. In eq. (2.9), all $R_{ii} = 0$ but both $R_{ij}$ and $R_{ji} = R_{ij}$ contribute. Physically, eq. (2.9) sums over all the pairwise interactions and divides this by the number of spins which share the relaxing magnetization. This assumes that each spin is interacting strongly with at least one neighbor. In nuclear spin relaxation jargon, this means that $R_2 \ll R$ where $R_2^{-1} = T_2$ is the spin–spin relaxation time.

This approach neglects the fact that several identical spins will form higher order nuclear spin species. For example, consider the three $I = 1/2$ protons in the $CH_3$ group in fig. 1. If higher-order spin species were formed, rather than being treated as three mutually interacting spin-1/2 pairs with six terms in eq. (2.9), the three spins should be treated as a single unit having $I = 1/2$ and $I = 3/2$ species [9]. This problem has been discussed thoroughly [4,9,11–13]. The four-spin-1/2 problem for $CH_4$ has also been discussed extensively [14,15].

The second assumption involves the manner in which the angular dependence of the relaxation process is treated. $R$ in eq. (2.6) depends on the various orientations of the spin–spin vector in the applied magnetic field via $\Omega = \theta^L, \phi^L$ in eq. (2.1). For a single crystal, there is a fixed number of such angles and for a macroscopic polycrystalline or glassy sample, there is, in effect, a continuous distribution of such angles. The appropriate averaging should be done with the magnetization in eq. (2.4), not with the relaxation rate in eq. (2.6) which is what we will do below. The relaxation process will, in general, be a sum of exponentials as opposed to a single exponential as expressed in eq. (2.5). Although we will begin by noting the explicit angle dependence for $R$, we will quickly perform an average appropriate for a polycrystalline or glassy sample.

The third assumption in the procedure leading to eq. (2.6) is that interesting results involving the combination of nuclear spin symmetry (whose neglect we are calling assumption one) and the correlated motions of three or more spins are neglected. If the motion of various $r$ vectors is correlated, $\Delta M$ will relax via a sum of exponentials and one must deal with cross correlation functions $J_{\mu\nu}$, $\mu \neq \nu$, as defined in eq. (2.7). For the three spins in a $CH_3$ group, for example, the motion of the three spin–spin vectors are perfectly correlated and a sum of four exponentials results. The angular dependencies introduced in the discussion of the second assumption play an important role in some cases [12,13,16–18].

The matters considered above are important, they are sometimes related, and they all lead, in principle, to nonexponential relaxation. Fortunately, they do not matter, in practice, for a large class of Van der Waals solids, although the effects have certainly been verified experimentally for carefully selected systems. Including these effects for the case of a spin–spin vector whose length is time-dependent results in an extremely complicated problem. Although this more general problem seems intractable at this time, with new sophisticated computer algebra programs it is a problem whose solution is on the horizon. To our knowledge, the matters raised in the three assumptions discussed above have only been investigated theoretically for groups of two, three and four spins. Experimentally, the predictions have been verified for $CH_3$ groups. The results for $CH_3$ groups show that if a time-dependent relaxation rate $R(t)$ is defined by

$$R(t) = -\frac{1}{\Delta M(0)} \left(\frac{\mathrm{d}\Delta M(t)}{\mathrm{d}t}\right) \qquad (2.10)$$

for the general case including all the effects discussed above, then in the limit that $t \to 0$, $R(t)$ in eq. (2.10) reduces to $R$ given by eq. (2.6). This has been verified experimentally and computationally for $CH_3$ groups [12,18]. Fortunately, where the relaxation is observed to be nonexponential, there is usually a well-defined initial decay in the observed $M(t)$ and $R \equiv R(0)$ is

usually well defined [19]. In this case, $R$ in eq. (2.6) is appropriate. In many cases, these three effects are not even observed, usually because many more than three or four spins are strongly coupled, or because the motion is not sufficiently anisotropic, or both. Even if the motion is highly anisotropic as in the case of a time-independent reorientation axis, a static but continuous distribution of reorientation axes will often mimic isotropic reorientation. For the case of random, isotropic hopping, eq. (2.6) results from the multi-spin strong coupling limit. The nonisotropic random reorientational motion we are considering is an enormous problem and one intuitively feels that when exponential relaxation is observed in a polycrystalline or glassy sample, eq. (2.6) is again valid. This is only a conjecture, however, and must be constantly tested by developing theoretical models and comparing these models with experiment. We will discuss these matters further as they arise.

## 3. Hopping models for molecular reorientation

### 3.1. The stochastic model

We consider a general class of models where the vector $r$ between two spins can take on $N$ values labeled $r_n$ for $1 \leqslant n \leqslant N$. We define $p(n, t)$ as the probability that $r$ takes on the value $r_n$ at time $t$. The $p(n, t)$ satisfy the Master Equation:

$$\frac{\mathrm{d}}{\mathrm{d}t}\, p(n, t) =$$

$$\sum_{\substack{m=1 \\ m \neq n}}^{N} W(m, n)p(m, t) - \sum_{\substack{m=1 \\ m \neq n}}^{N} W(n, m)p(n, t),$$

$$\hspace{11cm} (3.1)$$

$1 \leqslant n \leqslant N$. $W(m, n)$ is the probability per unit time for the spin–spin vector $r$ to hop from $r_m$ to $r_n$ ($m \neq n$). The $p(n, t)$ satisfy the normalization

$$\sum_{n=1}^{N} p(n, t) = 1 \qquad (3.2)$$

for all times $t$.

We now restrict ourselves to an important class of motions where all the relative positions of the spins (i.e. all $r_n$) are equally likely. This is equivalent to saying that all the allowed positions for the intramolecular unit or the molecule or the molecules (if the two spins are on different molecules) are equally likely. That is, each of the positions $r_n(t), 1 \leq n \leq N$, for a pair of spins corresponds to the same minimum in the spatially dependent electrostatic potential energy function. This is the case for the example in fig. 1 if methyl reorientation is the only motion. It follows that there is no preferred final state:

$$p(n, \infty) = \frac{1}{N}, \qquad (3.3)$$

for all $1 \leq n \leq N$. The correlation function $\langle F_\mu^*(0) F_\nu(t) \rangle$ in eq. (2.7) [2,3,20] is

$$\langle F_\mu^*(0) F_\nu(t) \rangle = \sum_{m=1}^{N} \sum_{n=1}^{N} F_\mu^*(r_m) F_\nu(r_n)$$
$$\times P(n, t; m, 0) p(m, 0), \qquad (3.4)$$

with $F_\mu$ given by eq. (2.8). $P(n, t; m, 0)$ is the conditional probability that the spin–spin vector $r$ takes on the value $r_n$ (i.e. that the system is in spatial state $n$) at time $t$ given that it had the value $r = r_m$ at $t = 0$. $P(n, t; m, 0)$ is obtained from $p(n, t)$ with the appropriate initial condition for $p(n, 0)$:

$$P(n, t; m, 0) = p(n, t) \quad \text{given that } p(n, 0) = \delta_{mn}, \qquad (3.5)$$

for all $1 \leq n, m \leq N$.

We have assumed that the conditional probabilities $P(n, t; m, 0)$ are independent of the choice of the time origin. The reorientation of the molecules is therefore a stationary process [21] whose correlation function $\langle F_\mu^*(0) F_\nu(t) \rangle$ is also stationary. This allows us to write eq. (3.4) for $\langle F_\mu^*(0) F_\nu(t) \rangle$. The summations in eq. (3.4) are over all possible initial and final spatial states (i.e. initial and final values of $r$). This approach is appropriate for discrete hopping models for the motion. For diffusion, the summations can be replaced by the appropriate integrals.

## 3.2. The molecular references frame

We will perform many of the needed calculations in a reference frame centered on the molecule of interest. This is the molecular-fixed frame (MFF) and is chosen such that it is time independent. We show MFF for 1-methyl-naphthalene in fig. 1. The same situation is appropriate to many methyl-substituted aromatic molecules including those discussed in section 6. In this case, the methyl ($CH_3$) group reorients about the C–C bond which is taken as the $z$-axis of MFF. In the solid state, the aromatic ring structure does not move on the nuclear magnetic resonance time scale.

Several geometric parameters are shown in fig. 2. Two values of $r$, namely $r_m$ and $r_n$, $1 \leq n, m \leq N$ are shown as well. The subscripts $m$ and $n$ label two of the allowed spin–spin vectors for the same pair of spins. The subscripts $m$ and $n$ do *not* label spins. There are only two spins under consideration, one of which is taken to be at the origin in fig. 2. The Euler angles $\Xi = \alpha, \beta, \gamma$
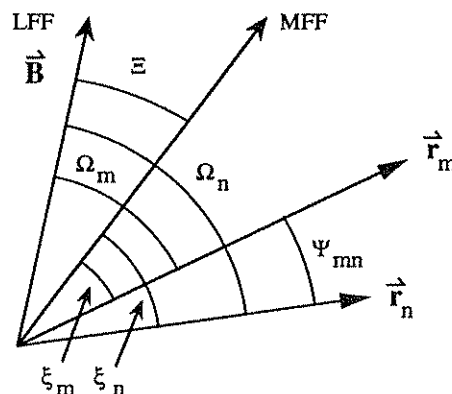


Fig. 2. Schematic representation of the reference frames, the vectors and the angles appropriate for the nuclear spin relaxation problem. LFF and MFF are the laboratory fixed reference frame and the molecular fixed reference frame. The $z$-axis of LFF is coincident with the applied magnetic field $B$. The orientation of MFF is determined by the geometry of the molecule. The Euler angles $\Xi = \alpha, \beta, \gamma$ specify MFF in LFF. The vectors $r_n$ and $r_m$ ($1 \leq m, n \leq N$) are two of the $N$ allowed spin–spin vectors for a single pair of spins, one of which is taken to be at the origin. The $r_n$ ($1 \leq n \leq N$) are specified by the polar and azimuthal angles $\Omega_n = \theta_n^L, \phi_n^L$ in LFF and by the Euler angles $\xi_n = \phi_n^M, \theta_n^M, \lambda_n^M$ in MFF. The frame-independent angle between $r_m$ and $r_n$ is $\psi_{mn}$.

specify MFF in LFF. The polar and azimuthal angles $\Omega_n = \theta_n^L, \phi_n^L$, with $1 \leq n \leq N$, specify $r_n$ in LFF. The Euler angles $\xi_n = \phi_n^M, \theta_n^M, \lambda_n^M$ specify $r_n$ in MFF. The frame-independent angle $\psi_{mn}$ is the angle between $r_m$ and $r_n$.

We transform the $Y_2(\Omega)$ in eq. (2.8) from LFF to MFF [8] via

$$Y_{2\mu}(\Omega) = \sum_{\delta=-2}^{+2} D_{\delta\mu}^{(2)}(\Xi) Y_{2\delta}(\xi) \qquad (3.6)$$

where $D_{\delta\mu}^{(2)}$ is the $\delta\mu$ component of a Wigner rotation matrix of rank two [8]. The correlation function in eq. (3.5) becomes

$$\langle F_\mu^*(0) F_\nu(t) \rangle = \sum_{m=1}^{N} \sum_{n=1}^{N} \mathcal{A}_{mn}^{\mu\nu} P(n, t; m, 0) p(m, 0) \qquad (3.7)$$

with

$$\mathcal{A}_{mn}^{\mu\nu} = \frac{8\pi}{15} r_m^{-3} r_n^{-3} \sum_{\delta=-2}^{+2} \sum_{\varepsilon=-2}^{+2} D_{\delta\mu}^{(2)}(\Xi) D_{\varepsilon\nu}^{(2)*}(\Xi)$$
$$\times Y_{2\delta}^*(\xi_m) Y_{2\varepsilon}(\xi_n) \qquad (3.8)$$

and the spectral density in eq. (2.7) becomes

$$J_{\mu\nu}(\omega) = \sum_{m} \sum_{n} \mathcal{A}_{mn}^{\mu\nu} \mathcal{J}_{mn}(\omega) \qquad (3.9)$$

with

$$\mathcal{J}_{mn}(\omega) = \int_{-\infty}^{+\infty} P(n, t; m, 0) p(m, 0) e^{-i\omega t} dt . \qquad (3.10)$$

We note that in the expression for $J_{\mu\nu}$ in eq. (3.9), the only dependence on $\mu$ and $\nu$ involves the $\Xi$-dependent matrices $D^{(2)}$ in eq. (3.8). As will be seen, the effects of cross correlations ($\mu \neq \nu$) and the manner in which the $\Xi$-dependence is handled are linked.

### 3.3. The sample average

For a solid composed of molecules with a motionless part (on the nuclear magnetic resonance time scale) on which MFF is anchored, the angles $\Xi$ which relate MFF and LFF will be time independent. For an isotropic liquid, $\Xi$ will be a random function of time for all molecules. For oriented liquids (i.e. liquid crystals) and some solids, like plastic solids, $\Xi$ will have a complicated time dependence. The problems of anisotropic motion in liquid crystals is much studied [22,23]. We are concerned with the solid state where the angles $\Xi$ are time independent. One can study a macroscopic single crystal with a set of known values for $\Xi$. Most experiments, however, have been performed on polycrystalline or glassy samples and we shall restrict ourselves to this case. As such, we assume an isotropic distribution of $\Xi$ relevant to a polycrystalline or glassy sample. This is referred to as a 'powder' average. For a glass, there is no long-range crystal structure. In a polycrystalline structure, however, the crystal structure will be preserved as long as each crystallite contains many unit cells. As an aside, for many organic molecules of interest with several distinct proton–proton vectors per molecule and several molecules per unit cell [24,25] we speculate that a powder average will be a very good approximation even for a single crystal.

For a macroscopic sample, the product

$$K(\Xi) \equiv D_{\delta\mu}^{(2)}(\Xi) D_{\varepsilon\nu}^{(2)*}(\Xi)$$

contained within eq. (3.8) with $\Xi \equiv \alpha, \beta, \gamma$ is replaced by

$$\bar{K} = \int_{0}^{2\pi} \int_{0}^{\pi} \int_{0}^{2\pi} D_{\delta\mu}^{(2)}(\alpha\beta\gamma) D_{\varepsilon\nu}^{(2)*}(\alpha\beta\gamma) \mathcal{P}(\alpha\beta\gamma)$$
$$\times d\alpha \sin\beta \, d\beta \, d\gamma . \qquad (3.11)$$

As stated above, one can use distribution functions $\mathcal{P}(\Xi)$ characteristic of specific single crystals, but here we invoke a powder average which gives an a priori equal distribution of angles $\Xi$ [8]:

$$\mathcal{P}(\alpha\beta\gamma) = \frac{1}{2} \frac{1}{2\pi} \frac{1}{2} , \qquad (3.12)$$

which gives

$$\bar{K} = \tfrac{1}{5}\delta_{\delta\varepsilon}\delta_{\mu\nu} \qquad (3.13)$$

where $\delta$ is the Kronecker delta symbol. Equation (3.8) becomes

$$\mathscr{A}^{\mu\nu}_{mn} = \delta_{\mu\nu}\,\frac{8\pi}{15}\,r_m^{-3}r_n^{-3}\,\frac{1}{5}\sum_\varepsilon Y^*_{2\varepsilon}(\xi_m)Y_{2\varepsilon}(\xi_n)\cdot \qquad (3.14)$$

We note that the powder average of the relaxation rate $R$ rather than of the magnetization which is, in principle, more appropriate as discussed previously, eliminates the need to consider cross correlations. However, this is only true in the final analysis because we have also neglected spin symmetry effects. These are important matters which are much discussed in the literature referenced above. The consequence of the combination of the three assumptions discussed above plus the powder average is that the relaxation rate is zero unless $\mu = \nu$ which means that cross correlations play no role.

The sum over $\varepsilon$ in eq. (3.14) can be simplified by the spherical harmonic addition theorem [8]:

$$\sum_{\varepsilon=-2}^{2} Y^*_{2\varepsilon}(\xi_m)Y_{2\varepsilon}(\xi_n) = \frac{5}{4\pi}\,\mathrm{P}_2(\cos\psi_{mn})\,, \qquad (3.15)$$

where $\mathrm{P}_2$ is the Legendre polynomial of order 2 and $\psi_{mn}$ is the angle between $r_n$ and $r_m$ (as shown in fig. 2) and defined explicitly by

$$\cos\psi_{mn} = \frac{r_m \cdot r_n}{r_m r_n}\,. \qquad (3.16)$$

The parameter $\mathscr{A}^{\mu\nu}_{mn}$ takes on the simple form

$$\mathscr{A}^{\mu\nu}_{mn} = \delta_{\mu\nu}\,\frac{2}{15}\,r_m^{-3}r_n^{-3}\mathrm{P}_2(\cos\psi_{mn})\,. \qquad (3.17)$$

Note that this expression is independent of the coordinate system.

## 4. The unrestricted hopping model

### 4.1. General theory

So far, we have not specified a model for the hopping process. In this paper we will investigate the unrestricted hopping model. For methyl reorientation in a three-fold potential, $r$ is allowed to hop from one position to any other allowed position. There are $N = 3$ positions. All hops are a priori equally likely. In this case,

$$W_{mn} = W \qquad (4.1)$$

for $1 \leqslant m, n \leqslant N, m \neq n$. The $N$ eqs. (3.1) are decoupled and reduce to

$$\frac{\mathrm{d}}{\mathrm{d}t}\,p(n, t) = W[1 - Np(n, t)]\,, \quad 1 \leqslant n \leqslant N\,, \qquad (4.2)$$

with solutions

$$p(n, t) = A_n + B_n\,\mathrm{e}^{-NWt}\,. \qquad (4.3)$$

The initial and final conditions in eqs. (3.3) and (3.5) give

$$P(n, t; m, 0) = \frac{1}{N} + \left(\delta_{mn} - \frac{1}{N}\right)\mathrm{e}^{-NWt}\,. \qquad (4.4)$$

$\mathscr{J}$ in eq. (3.10) is

$$\mathscr{J}_{mn}(\omega, NW) =$$
$$\frac{1}{N^2}\,\delta(\omega) + \frac{1}{N}\left[\delta_{mn} - \frac{1}{N}\right]j(\omega, NW)\,, \qquad (4.5)$$

with the reduced spectral density given by

$$j(\omega, NW) = \frac{2NW}{(NW)^2 + \omega^2}\,. \qquad (4.6)$$

The entire procedure leading to a value of $R$ given by eq. (2.6) is based on a perturbation treatment of the spin–lattice and spin–spin interactions and it is only valid in the high-magnetic-field limit. In practice this means that the Zeeman field $B = \omega/\gamma$ must be much larger than the local dipolar fields. Thus the procedure is not valid for $\omega = 0$ and the term with $\delta(\omega)$ in eq. (4.5) can be dropped.

Finally, we write the relaxation rate in eq. (2.6) as

$$R = \frac{1}{5} \left( \frac{\mu_0}{4\pi} \right)^2 \gamma^4 \hbar^2 I(I+1) A \rho^{-6} q(\omega, NW) \quad (4.7)$$

with

$$A = 1 - \frac{15}{2N^2} \rho^6 \sum_{m=1}^{N} \sum_{n=1}^{N} \mathscr{A}_{mn} , \quad (4.8)$$

$$\rho^{-6} = \frac{1}{N} \sum_{m=1}^{N} r_m^{-6} , \quad (4.9)$$

and

$$q(\omega, NW) = j(\omega, NW) + 4j(2\omega, NW) . \quad (4.10)$$

The definitions of $A$ and $\rho$ are very useful. Equation (4.7) retains the (famous) factor $1/5$ whose origin is in the powder average in eq. (3.13). The distance parameter $\rho$ is just an appropriate average over the distances since the spin–spin separation enters the hamiltonian in eq. (2.1) as $r^{-3}$ and this is squared in $R$ (i.e. from perturbation theory). If the $N$ values of $r = |r_n|$ are equal then $\rho = r$. If the smallest value of $r_n = |r_n|$ (call it $r_{\min}$) is much smaller than any of the other $N-1$ values then $\rho \simeq r_{\min}$. The parameter $A, 0 \leqslant A \leqslant 1$, measures the effect of the angles $\psi_{mn}$ between the spin–spin vectors. Palmer has discussed the mathematics of the parameters $A$ and $\rho$ in detail as well as the physical insight they give into the use of the general theory in complicated but realistic geometries [26].

### 4.2. Hopping models for N = 1, 2 and 3

If $N = 1$ there is only one spin–spin vector $r_1$. There is no motion, the spin–spin hamiltonian in eq. (2.1) is not modulated and the relaxation rate is zero. For $N = 2$ and 3 the unrestricted hopping model developed here will always be appropriate since every other available geometric state is a nearest neighbor. For $N > 3$, a more realistic model may be needed whereby the spin-spin vector is restricted regarding to which of the $N$ positions it can hop.

Our model assumes that all $N$ values for $r_n$ are equally likely. Others have studied the $N = 2$

case for the more general situation where the two spatial states correspond to different electrostatic potential energies [27,28]. Palmer has shown that eq. (4.7) with $N = 2$ reduces to the expression which these more general approaches generate when the electrostatic energy between the two spatial states is set to zero [26].

The case of $N = 3$ is relevant because of the importance of methyl group rotation in many branches of physics and chemistry. The relaxation rate in eq. (4.7) reduces to the well-known expressions for relaxation due to intramethyl interactions when all three values of $|r_n|$ are set equal. This is shown below as a special case of reorientation on a regular polygon.

It is theoretically useful and physically informative to treat the case of general $N$ even though we will only use $N = 3$ in this paper.

### 4.3. Reorientation on a regular polygon

In this case, the motion of a pair of spins is such that the spin–spin vector $r$ can assume $N$ values distributed on a regular polygon, part of which is shown in fig. 3. The two-dimensional hopping motion takes place about an axis perpendicular to the plane of spin positions and the vector $r$ reorients on a regular polygon. All $N$ values of $r_n$ have the same length. The angles between neighboring $r_n$ are $\alpha = 2\pi/N$ as shown in fig. 3. Since the vector $r$ can jump to any other place on the polygon, the allowed angles between vectors $r$ are $\psi_{mn} = (m - n)(2\pi/N)$ for $1 \leqslant m, n \leqslant N, m \neq n$. This is the $\psi_{mn}$ shown in fig. 2. For all the vectors $|r_n| = r$. The calculation of the $\mathscr{A}_{mn}$ in eq. (3.17) and $A$ in eq. (4.8) is straightforward, if somewhat tedious. $R$ for the unrestricted hopping model is given by eq. (4.7)
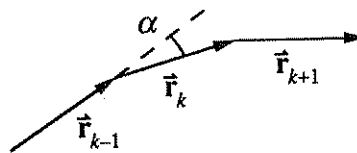


Fig. 3. Reorientation on a regular polygon. Three of the $N$ vectors $r_n$ are shown. The angle between $r_k$ and $r_{k-1}$ is $\alpha$ for all $1 \leqslant k \leqslant N$.

with $\rho = r$ and $A = 3/4$. The geometric part of $R$ is found to be *independent of N*. Indeed, if an $N$-independent correlation time $\tau$ is associated with $(NW)^{-1}$ in eq. (4.6), the result is completely independent of $N$. The probability $W$ or $NW$ needs to be modelled, though we do not address this important problem here.

### 4.4. The intramethyl relaxation rate

The above result is immediately applicable to the determination of the relaxation rate due to the intramethyl interactions in a methyl group. The relaxation rate resulting from methyl group reorientation about the threefold axis, considering only the intrametyl interaction between two of the protons, is

$$R_0 = S_0 q(\omega, 3W) \tag{4.11}$$

where $S_0 = 1.9 \times 10^9 \text{ s}^{-2}$ is given by

$$S_0 = \frac{3}{20} \left( \frac{\mu_0}{4\pi} \right)^2 \gamma^4 \hbar^2 I(I+1) r^{-6} \tag{4.12}$$

with $I = 1/2$, $\gamma = 2.675 \times 10^8 \text{ kg}^{-1} \text{ s A}$ and $r = 0.180 \text{ nm}$, the proton–proton separation in a methyl group.

The relaxation rate for an ensemble of *isolated methyl groups* is obtained by using eq. (2.9) and noting that there are *six* mutual interactions among the three spins. Thus, $R^{\text{methyl}} = (6/3)R_0$, a well-known expression for a relaxing methyl group [4,5,29]. A typical $\omega$ might be $2\pi \times (50 \text{ MHz})$ and when $3W$ is in this range, $j$ in eq. (4.6) is $j = \omega^{-1}$ and $R^{\text{methyl}} = 17 \text{ s}^{-1}$. Finally, if only intramethyl interactions are considered in a molecule with $m$ independent and noninteracting methyl groups and $M$ protons, the *observed* relaxation rate is given by $R = m(6/M)R_0 = (3m/M)R^{\text{methyl}}$. The factor $3m/M$ is often referred to as the ratio of 'relaxing' to 'nonrelaxing' protons but this is a confusing terminology since the origin of the factor 3 does not lie solely in the fact that there are three protons in a methyl group and the origin of the factor $M$ is that all the protons are relaxing!

### 4.5. Reorientation on a right circular cone

This is a generalization of reorientation on a polygon. In the reference frame of one of the two spins, the other spin hops among the $N$ positions on a circle as shown in fig. 4 where the angles $\phi_{mn}$ and $\delta$ are defined. This geometry preserves the condition that $|r|$ is constant and finds very restricted use in practice. An example would be the interaction between a methyl proton in the 1-methyl group and the proton in the 4-position in methylbenzene or 1-methylnaphthalene (fig. 1). The $r$ is sufficiently large in this case that this interaction does not really matter. However, as a theoretical development, $r$ reorients in three dimensions, and this case is an important bridge between simpler cases like hopping on a regular polygon where $r$ reorients in two dimensions as discussed above, and more general models where $r$ hops in three dimensions and $|r|$ changes with time. The angles $\psi_{mn}$ are given by $\cos \psi_{mn} = \cos^2\delta + (\sin^2\delta)(\cos \phi_{mn})$. The angle $\delta$ is determined by the geometry of interest and the angles $\phi_{mn} = (m - n)(2\pi/N)$ for $1 \le m, n \le N$ as in the case of reorientation on a regular polygon presented in section 4.3. $R$ is given by eq. (4.7) with $\rho = r$ and $A = \frac{3}{4}(\sin^4\delta + \sin^2 2\delta)$. Reorientation on a polygon is obtained by setting $\delta = 90°$ in which case $A = 3/4$ as determined above. This expression for $R$ can be obtained from, and is in agreement with, previously derived analogous expressions for $R$ for the case of a methyl group undergoing various
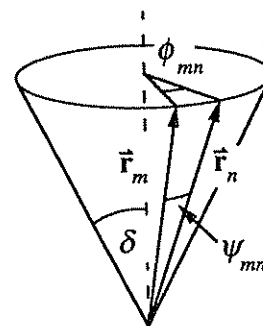


Fig. 4. Reorientation on a right circular cone. The spin–spin vector $r$ can be in any of $N$ orientations equally spaced on a right circular cone of half-angle $\delta$. Shown are two such orientations, $r_m$ and $r_n$, separated by an angle $\psi_{mn}$. The azimuthal angle between the two vectors is $\phi_{mn}$.

superimposed reorientations [9, 30]. Many of these previous calculations are cumbersome and they only correspond to $N = 3$. Within the confines of the limits of the present unrestricted hopping model and the particular geometry, plus the limits of applicability resulting from the assumptions inherent in the whole approach, the results presented here is valid for any $N$.

## 4.6. Reorientation on an oblique cone

We consider the geometry shown in fig. 5. One spin hops in a plane and the other is 'fixed' anywhere in space. The former can belong to a methyl group for $N = 3$ and the latter can be a non-methyl spin somewhere else in the molecule or on a neighboring molecule.

All preceding cases can be considered as subsets of this case so it is important to note that by 'fixed' we mean either that a spin is truly fixed in space relative to the applied Zeeman field or that it is possible to translate each $r_n(t)$ separately such that the $N$ vectors have a common origin. This must be done in such a way that the $N$ values of $r_n(t)$ in a time-independent molecular-fixed reference frame remain unchanged. For example, if both spins are in a methyl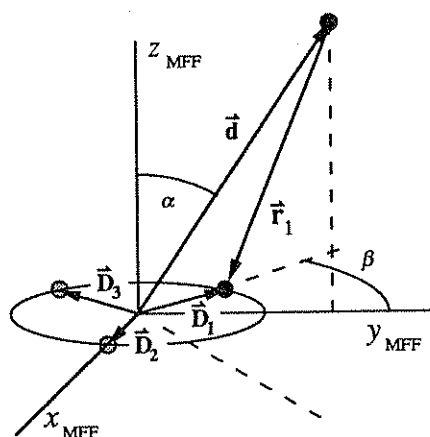 group then they are both moving but their motion is perfectly correlated, and it is immaterial whether the $r_n$ are depicted in the 'physical' picture as in the methyl group in fig. 1 or in the reference frame of one of the spins as in fig. 5 with $d = 0$. In both cases the local time-independent molecular fixed frame (MFF) is the same. On the other hand, the interaction between two protons on different methyl groups with arbitrary relative orientations does not satisfy this condition. It is an important restriction, then, that in the time-independent molecular-fixed reference frame, the position of the 'fixed' spin can be *considered* time independent.

The origin of MFF is the center of the polygon formed by the $N$ positions of the 'mobile' spin. The $N$ *positions* lie in the $x$–$y$ plane and the 'fixed' spin lies in the $y$–$z$ plane. The $N$ vectors $D_n$ specify the $N$ positions for the *single* mobile spin and $d$ specifies the position of the *single* fixed spin. The spin–spin vectors $r_n$ are $r_n = D_n - d$. The angle $\alpha$ is the azimuthal angle specifying the fixed spin in MFF. The angle $\beta$ is the angle in the $x$–$y$ plane between the projection of $d$ onto the $x$–$y$ plane (which is the $y$ axis) and the *nearest* mobile spin position. Thus, $0 \leqslant \beta \leqslant \pi/N$. For a specific interaction in a particular molecule, the angle $\alpha$ and the distance $d$ are independent of the motion. The vectors $d$ and the $D_n$ can be expressed in terms of $d$, $D$, $\alpha$ and $\beta$, where we note that $D = |D_n|$ is independent of $n$. We present the example appropriate to the $N = 3$ situation which would characterize the interaction between a methyl group proton and a non-methyl group proton. In this case,

$$r_1 = (D - d \sin \alpha \cos \beta)\hat{x}$$
$$- d \sin \alpha \sin \beta \, \hat{y} - d \cos \alpha \, \hat{z},$$

$$r_2 = -\left(\frac{1}{2} D + d \sin \alpha \cos \beta\right)\hat{x}$$
$$+ \left(\frac{\sqrt{3}}{2} D - d \sin \alpha \sin \beta\right)\hat{y} - d \cos \alpha \, \hat{z},$$

$$r_3 = -\left(\frac{1}{2} D + d \sin \alpha \cos \beta\right)\hat{x}$$
$$- \left(\frac{\sqrt{3}}{2} D + d \sin \alpha \sin \beta\right)\hat{y} - d \cos \alpha \, \hat{z}.$$

$$(4.13)$$

Fig. 5. The oblique cone geometry. The fixed spin is in the $y$–$z$ plane and its position is specified by $d$ which makes an angle $\alpha$ with the $z$-axis of the molecular-fixed frame (MFF). The $N$ positions of the mobile spin are specified by $D_n$ in MFF. The case $N = 3$ is shown. The angle between the projection of $d$ onto the $x$–$y$ plane (which will be the $y$ axis) and the *nearest* $D_n$ is $\beta$. As such, $0 \leqslant \beta \leqslant \pi/N$.

The triad $\hat{x}$ $\hat{y}$ $\hat{z}$ specifies MFF. The $r_n = |r_n|$ are then computed as in $\rho$ in eq. (4.9). The $\psi_{mn}$ are computed from eq. (3.16). A useful dimensionless parameter is

$$w = \frac{D}{d} \qquad (4.14)$$

which, for $N = 3$, allows $\rho$ to be expressed as

$$\rho^{-6} = \tfrac{1}{3} d^{-6} [(1 - 2w \sin \alpha \cos \beta + w^2)^{-3}$$
$$+ (1 + w \sin \alpha (\cos \beta - \sqrt{3} \sin \beta) + w^2)^{-3}$$
$$+ (1 + w \sin \alpha (\cos \beta + \sqrt{3} \sin \beta) + w^2)^{-3}].$$
$$(4.15)$$

We note that this expression is invariant for $\alpha \rightarrow \pi - \alpha$ and triply periodic in $\beta$ in the range $0 \leqslant \beta \leqslant 2\pi$ since the numbering of the three vectors does not matter.

Although we have used $N = 3$ as an example in the above expressions, it is straightforward, if somewhat time-consuming for most small computers, to generate these expressions for higher values of $N$ using *Mathematica*.

## 5. Methyl-ring interactions

### 5.1. The general procedure

We now restrict ourselves to the case of $N = 3$ and develop the relaxation rate resulting from the interaction between a *single* methyl group proton and a *single* ring proton in methyl-substituted planar aromatic molecules using the geometry of an oblique cone. In section 6, we will sum the various contributions developed here to obtain the total (observed) relaxation rates for real molecules and then compare these results with experimentally determined parameters where possible. We assume an ideal geometry. Methyl C–H, ring C–H, ring C–C and ring-methyl C–C bond lengths are [31,32] 0.110 nm, 0.108 nm, 0.140 nm and 0.150 nm. All angles involving the ring are 120° and all angles in the methyl group are $\cos^{-1}(-1/3) = 109.47°$. The vectors $d$, $D_i$ and

the angle $\alpha$ may now be specified for a particular interaction. The length $|D_i| = D = 0.1037$ nm is characteristic of a methyl group and so is common to all the cases considered here.

The angle $\beta$ depends on the orientation of the methyl group and we will treat this as a variable. This will be especially valuable when the theoretical results are compared with experimentally determined parameters. The fixed spin is on the $y$–$z$ plane in the aromatic ring. It is important to remember that $\beta$ specifies the methyl proton position nearest the fixed spin. The fixed spin will always be in the $y$–$z$ plane. Thus, for example, in fig. 1, all three protons in the methyl group are characterized by $\beta = 0$ for the ortho interaction and by $\beta = 60°$ for the peri interaction. So, even though $\beta$ depends on the orientation of the methyl group, it should not be used to specify the orientation of a methyl group since $\beta$ will take on different values for different interactions for the same methyl group orientation.

We determine $\alpha$, then $d$, then the vectors $r_n(\beta)$ in eq. (4.13). The ratio $w$ in eq. (4.14) is determined as is the distance function $\rho(\beta)$ in eq. (4.15). The angles $\psi_{mn}$ in eq. (3.16) follow, or at least the values of $P_2(\cos \psi_{mn})$. The $\mathcal{A}_{mn}$ in eq. (3.17) are then determined. The parameter $A$ in eq. (4.8) is computed and the relaxation rate in eq. (4.7) is expressed in algebraic, numerical or graphical form using *Mathematica*. We note that using *Mathematica*, exact algebraic expressions for the relaxation rate can be produced. However, these are usually very lengthy and offer little insight. A plot and a subsequent representation by a simple fitted function is usually much more informative.

### 5.2. The methyl-ortho interaction

The methyl-ortho interaction refers to the interaction between a single methyl proton and a neighboring proton on the same ring. For example, the 2-proton in fig. 1 is an ortho proton. Figure 1 shows $\beta = 0$ for this interaction but we calculate $R$ as a function of $\beta$. In this case we determine that $\alpha = 46.7°$ and that $d = 0.295$ nm. The ratio $w$ is 0.351. The relaxation rate is

$$R_{\text{ortho}} = S_{\text{ortho}}(\beta)q(\omega, 3W) \tag{5.1}$$

and $S_{\text{ortho}}(\beta)$ versus $\beta$ is shown as a solid line in fig. 6. We can approximate the $\beta$-dependence of all the relaxation rates by a series expansion in $\cos(3m\beta)$, $m = 0, 1, 2, \ldots$. For $S_{\text{ortho}}$, a two-term fit is sufficient, giving

$$S_{\text{ortho}}(\beta) = (7.09 \times 10^7 \, \text{s}^{-2})$$
$$+ (1.94 \times 10^7 \, \text{s}^{-2}) \cos(3\beta) \tag{5.2}$$

which is shown as a dashed line in fig. 6. We have chosen to make the approximation exact for the maxima and the minima, that is, for $\beta = 0$ and for $\beta = 60°$. The error at 30° is about 3%. As discussed above, $0 \leqslant \beta \leqslant 60°$, and we present $0 \leqslant \beta \leqslant 180°$ in fig. 6 to show the expected periodicity. In real molecules, we expect to find $\beta = 0$, 30° or 60° depending on what atom or atomic group is attached to the ring on the other side of the methyl group. Palmer has tabulated the parameters $r_1, r_2, r_3$, $\psi_{12}, \psi_{13}, \psi_{23}$, $A, S_{\text{ortho}}$ and $S_{\text{ortho}}/S_0$ for these three values of $\beta$ [26]. The ratio $S_{\text{ortho}}/S_0 = 0.046$, 0.036 and 0.027 for $\beta = 0$, 30° and 60°. $S_0$ is defined in eq. (4.12). These ratios are relevant because relaxation due to intramethyl interactions, characterized by $S_0$,
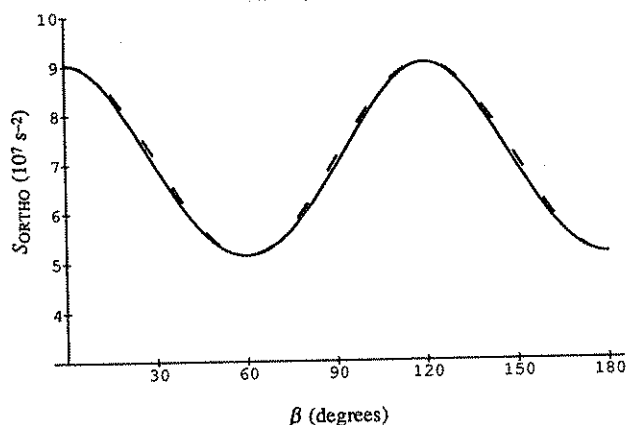


Fig. 6. $S_{\text{ortho}}$ vs $\beta$ for the methyl-ring ortho interaction. The solid line is the exact result and the dashed line is an approximation given by eq. (5.2). In practice, $0 \leqslant \beta \leqslant 60°$ but $0 \leqslant \beta \leqslant 180°$ is shown to display the symmetry. $\beta = 0$ corresponds to a methyl position lying in the aromatic plane adjacent to the ortho ring proton which is the case shown in fig. 1.

will always be present unless two of the three methyl protons are replaced by deuterons. The primary reason that these ratios are so small is that the ratio $\rho^{-6}/r_0^{-6}$ is very small.

### 5.3. Other methyl-single ring interactions

We have determined $R$ for the methyl-ring meta and methyl-ring para interactions. For the meta interaction, $\alpha = 25.5°$, $d = 0.499$ nm and $w = 0.208$. The relaxation rate is qualitatively similar to fig. 6 with

$$R_{\text{meta}} = S_{\text{meta}}(\beta)q(\omega, 3W) \tag{5.3}$$

and with

$$S_{\text{meta}}(\beta) = (7.38 \times 10^5 \, \text{s}^{-2})$$
$$+ (2.75 \times 10^4 \, \text{s}^{-2}) \cos(3\beta) \tag{5.4}$$

being an excellent approximation. The maximum value of $S_{\text{meta}}$ is 0.0004 of $S_0$ and can be neglected for a fully protonated methyl group. This is an important new result. This interaction would only be important when two of the three protons in a methyl group have been replaced by deuterons.

For the para interaction, $\alpha = 0$ and the relaxation rate is independent of $\beta$. This is a special case of an oblique-cone geometry which we have previously discussed and called a right circular cone geometry. For this case, $d = 0.575$ nm and $w = 0.180$, $\rho = r_1 = r_2 = r_3 = 0.584$ nm, $\psi_{mn} = 17.7°$ for $m \neq n$ and $R = S_{\text{para}}q(\omega, 3W)$ with $S_{\text{para}} = 1.99 \times 10^5 \, \text{s}^{-2}$ which makes $R_{\text{para}}$ completely negligible when compared with $R_{\text{methyl}}$ or even with $R_{\text{ortho}}$.

### 5.4. The methyl-peri interaction

The geometry for the methyl-peri interaction is shown in fig. 1. In this case, $\alpha = 72.0°$, $d = 0.255$ nm and $w = 0.407$. The procedure is as discussed above but the relaxation rate is much larger here than for the ortho, meta or para interactions. As before,
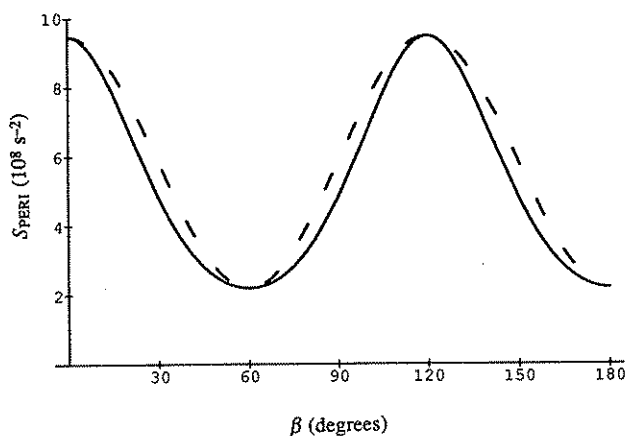
Fig. 7. $S_{peri}$ vs $\beta$ for the methyl-ring peri interaction. The solid line is the exact result and the dashed line is a two-term approximation. A three-term approximation given by eq. (5.6) is indistinguishable from the solid line. In practice, $0 \leqslant \beta \leqslant 60°$ but $0 \leqslant \beta \leqslant 180°$ is shown to display the symmetry. $\beta = 0$ corresponds to a methyl proton position lying in the aromatic plane adjacent to the peri ring proton. The case of $\beta = 60°$ is shown in fig. 1.

Table 1
Parameter values for the methyl-ring peri interaction for specific values of $\beta$.

| | $\beta = 0$ | $\beta = 30°$ | $\beta = 60°$ |
|---|---|---|---|
| $r_1$ (nm) | 0.160 | 0.179 | 0.225 |
| $r_2$ (nm) | 0.318 | 0.275 | 0.225 |
| $r_3$ (nm) | 0.318 | 0.345 | 0.355 |
| $\rho$ (nm) | 0.191 | 0.212 | 0.239 |
| $\chi_{12}$ (°) | 21.8 | 40.0 | 47.1 |
| $\chi_{13}$ (°) | 21.8 | 15.9 | 25.3 |
| $\chi_{23}$ (°) | 32.9 | 31.1 | 25.3 |
| $A$ | 0.531 | 0.513 | 0.484 |
| $S_{PERI}(\beta)$ (s$^{-2}$) | $9.46 \times 10^8$ | $4.79 \times 10^5$ | $2.19 \times 10^8$ |
| $S_{PERI}(\beta)/S_{PERI}(0)$ | 1.00 | 0.51 | 0.23 |
| $S_{PERI}(\beta)/S_0$ | 0.50 | 0.25 | 0.12 |

$$R_{peri} = S_{peri}(\beta)q(\omega, 3W \qquad (5.5)$$

with $S_{peri}(\beta)$ versus $\beta$ given in fig. 7. A two-term approximation to the exact curve is shown in fig. 7 as a dashed line but it is a poor representation. We present a three-term approximation which is indistinguishable from the exact curve at the level of precision presented in fig. 7:

$$S_{peri}(\beta) = (5.31 \times 10^8 \text{ s}^{-2})$$
$$+ (3.63 \times 10^8 \text{ s}^{-2}) \cos(3\beta)$$
$$+ (5.17 \times 10^7 \text{ s}^{-2}) \cos(6\beta) . \qquad (5.6)$$

This is an important interaction for many molecules and in table 1 we present the parameters that enter the problem.

### 5.5. Other methyl-distant ring interactions

Palmer has considered many interactions between a methyl proton and the protons at various positions on distant rings [26]. They present interesting exercises in computation and important checks in software development but they are completely negligible compared with other interactions that will always be present. However, since these interactions are contained in the appropriate *Mathematica* Notebooks, they can be automatically included in any computation of a whole-molecule relaxation rate.

## 6. The relaxation rate in real molecules

### 6.1. Experimental considerations

Experimental relaxation rates are usually presented as relaxation rate $R$ versus temperature $T$ (or more precisely $\ln R$ versus $T^{-1}$) for one or more frequencies $\omega$. The hop rate $NW$ in eq. (4.6) is usually modelled via an Arrhenius relationship $NW = \nu_\infty \exp(-E/kT)$ which introduces an activation energy $E$ and an infinite temperature hop rate $\nu_\infty$. The data fitting procedures for methyl rotation models are discussed extensively elsewhere [19,29,30]. In some cases, it is very difficult to compare the calculations presented here with experimental results for methyl-substituted planar aromatic molecules. First, the barrier $E$ is often not unique due to either the complexities of the crystal structure or to the presence of a glassy state (or both). In this case, the spectral density in eq. (4.6) is replaced by an appropriate distribution of such spectral densities [1] and the data can often still be meaningfully fitted provided both the long ($NW \ll \omega$) and the short ($NW \gg \omega$) correlation time limits, corresponding to low and high temperature respec-

tively, are experimentally investigated. Second, intermolecular spin–spin interactions can be important in some systems and we have not taken these into account. As a result, the theoretical results presented here can now help determine more accurately how important these interactions are. Third, the activation energy $E$ can be quite small for methyl reorientation and this means that quantum mechanical tunnelling at lower temperatures can play a role [33]. Fourth, sometimes, there are other motions such as whole-molecule rotation in the solid state, particularly for some of the smaller molecules. In spite of these four problems, this is the simplest class of molecules for which the theory presented here can be meaningfully applied and some interesting and useful results follow.

The experiments are analyzed using

$$R = Aq(\omega, 3W) \tag{6.1}$$

where $q(\omega, 3W)$ is given by eq. (4.10). The values of $A, E, \nu_\infty$ and, for more complicated models [1], other parameters as well, are determined from the experiment. We are only concerned with the value of the experimentally determined strength parameter $A$ in this work. Until now, $A$ has been compared with theoretical values that consider intramethyl interactions only; that is, with $6mS_0/M$ for $m$ methyl groups, $M$ total protons and $S_0 = 1.9 \times 10^{10}\,\text{s}^{-2}$ given by eq. (4.12). Now $A$ can be compared with a theoretical value which considers all appropriate intramolecular interactions and we do this at the end of the next section. Our main goal here is to present clearly the theoretical results in a manner which can be used to interpret experimental data, thus aiding in the determining of equilibrium geometries and in the development of dynamical models.

### 6.2. α-methyl substituted molecules

We present a calculation of the relaxation rate in α-methyl systems like 1-methylnaphthalene shown in fig. 1. For the present we consider only single methyl-substituted molecules but we consider *all* intramolecular spin–spin interactions.

We assume that methyl reorientation is the only motion on the nuclear magnetic resonance time scale. For $M$ protons in the molecule there will be $M(M-1)$ terms in eq. (2.9). There are six intramethyl interactions and $6(M-3)$ methyl-ring interactions. $M-3$ is the number of ring protons. The remaining $(M-3)(M-4)$ ring–ring interaction terms in eq. (2.9) are identically zero since only the methyl group is moving. That, is, the ring–ring interactions are not modulated.

$R$ is written in the form

$$R = \frac{1}{M}\left[6S_0 + S(\phi)\right]q(\omega, 3W). \tag{6.2}$$

$S_0$ corresponds to a single intramethyl interaction so $6S_0$ accounts for all six of them. $S(\phi)$ corresponds to all the methyl-ring interactions. The $6S_0 = 1.14 \times 10^{10}\,\text{s}^{-2}$ term usually dominates $6S_0 + S(\phi)$ and the methyl-ring peri interaction usually dominates $S(\phi)$. The angle $\phi$ specifies the orientation of the methyl group defined such that $\phi = 0$ in fig. 1. Thus $\phi = 0$ corresponds to $\beta = 0$ for the methyl-ortho interaction and $\beta = 60°$ for the methyl-peri interaction. Each of the $6(M-3)$ methyl-ring terms in $S(\phi)$ is then characterized by $\alpha, \beta$ and $w$. Since each methyl proton can assume the same three positions and since each proton pair contributes twice to the sum, these terms naturally divide into $M-3$ sets with each set having six terms. A separate *Mathematica* Notebook is produced for each of the $M-3$ sets since the specific geometries will occur in many other molecules. After many individual contributions to $S(\phi)$ have been computed they can be put together to generate the final relaxation rate. The total relaxation rate is then produced numerically or graphically as a function of the angle $\phi$. Although no algebraic expression is actually outputted at this stage, we emphasize that exact algebraic expressions are resident in computer memory and exact numerical values can be determined for any angle $\phi$.

For 1-methylnaphthalene (1-MN) shown in fig. 1, we write $R = S_{1\text{-MN}}(\phi)q(3W)$ with $S_{1\text{-MN}} = (1/M)[6S_0 + S(\phi)]$. $S_{1\text{-MN}}$ versus $\phi$ is shown in fig. 8. For $\phi = 0°$, $S(0) = 0.19 \times 10^{10}\,\text{s}^{-2}$ which is
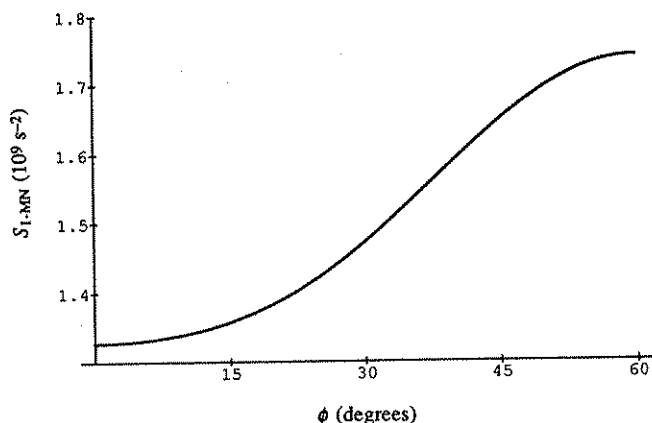
Fig. 8. Relaxation strength $S_{1\text{-MN}}$ versus methyl group orientation $\phi$. The value $\phi = 0$ corresponds to the orientation shown in fig. 1.

17% of $6S_0$ and 14% of the total $6S_0 + S(0)$. This is the orientation shown in fig. 1. As stated above, this is dominated by the peri interaction. The other interactions contribute less than 1% of the total. For $\phi = 60°$, a methyl proton is very near the peri proton and $S(60°) = 0.60 \times 10^{10}$ s$^{-2}$ which is 53% of $6S_0$ and 34% of the total $6S_0 + S(60°)$.

To better than 1%, the results for 1-methyl-phenanthrene, 9-methylphenanthrene and 1-methylanthracene are identical to the result for 1-methylnaphthalene. Only $M$ changes. This is not surprising in light of the fact that the methyl–non-methyl interactions that differ among these molecules contribute negligibly to the relaxation.

We can easily extend these results to molecules with more than one methyl group so long as it is reasonable to neglect the interactions between protons on different methyl groups. Our current model does not deal with more than one reorienting unit. This will be a good approximation as long as methyl groups are not adjacent. If $m$ groups are chemically identical (which is easily determined from the $R$ versus $T$ data) then all the appropriate terms in the expression are multiplied by $m$. If two or more methyl groups are chemically inequivalent then the 'other' methyl groups have an $NW$ very different from the methyl group of interest and they simply add to $M$, the total number of protons in the molecule.

$R$ versus $T$ experiments have been performed with 1,3-dimethylnaphthalene [34], 1,5-dimethylnaphthalene [34,35], 1,7-dimethylnaphthalene [34], 1-methylanthracene [36], 9-methylphenanthrene [29], 1,9-dimethylphenanthrene [37] and 3,9-dimethylphenanthrene [29]. Measurements have also been performed with 1-methyl-naphthalene itself [34,38] but unfortunately these cannot be interpreted because there is clearly an additional motion at high temperatures which renders the fitting procedure for methyl rotation parameters suspect, at best. The 1-, 4- and 5-positions in the methylnaphthalenes, the 1-position in 1-methylanthracene and the 1- and 9-positions in the methylphenanthrenes are all $\alpha$ methyls. Also, no two of the methyl groups in these molecules are adjacent. As suggested above, the methyl–methyl spin–spin interactions in these molecules are negligible because the spins are just too far apart. Thus we can consider all the molecules presented above with suitable changes to eq. (6.2). For consistency, we have previously reanalyzed all the data not from our laboratory [29]. The fitted values of $A$ where $A$ is the experimentally determined value of the strength parameter presented in section 6.1, is traditionally compared with $6S_0/M$ (or its equivalent for more than one methyl group) and the values $AM/(6S_0)$ range from 0.9 to 1.2 in the dimethyl-anthracenes [29] and they are all about unity in 1-methylanthracene [29] and in the methylphenanthrenes [29,37]. The experimental uncertainties in these parameters are about ±10% in the phenanthrenes and about ±20% in the naphthalenes and the single anthracene. If these values $AM/(6S_0)$ are replaced by $AM/(6S_0 + S(\phi))$ then the new values show unequivocally that for the real molecules, $\phi = 0$ (or nearly so), as expected. Since $S(60°)/(6S_0)$ is 0.53 and $S(0)/(6S_0)$ is only 0.17, the experimentally determined values $AM/(6S_0 + S(\phi))$ would be considerably less than unity if $\phi$ were near 60°. The fitted value of $AM/(6S_0 + S(\phi))$ can be larger than one since the denominator does not consider intermolecular interactions but it cannot be less than one (within the experimental uncer-

tainty and within the confines of the dynamical model) since the interactions considered in the denominator of this value are certainly present. The result that $\phi = 0$ or nearly so in these several molecules (with 1-methylnaphthalene not being among them) is in agreement with both ab initio calculations [39] and recent laser jet spectroscopy experiments for 1-methylnaphthalene [40]. Thus, it can now be said, for the first time, that solid state proton spin relaxation experiments have shown that $\phi = 0$ (or nearly so) in these molecules. Laser jet spectroscopy experiments are very difficult on large molecules and this new clear statement that $\phi = 0$ for the anthracenes and the phenanthrenes is the only clear determination of the orientation of the methyl group in these systems.

## 7. Summary

We have investigated the nuclear spin-lattice relaxation process in the case where the *lengths* of the spin–spin vectors $r$ change with time. We began with a general expression for the relaxation rate $R$, reviewing carefully the assumptions going into the derivation, particularly those which resulted in exponential relaxation. From there, we developed a stochastic model for molecular reorientation in polycrystalline or glassy samples. We assumed an unrestricted hopping model where $r$ could hop among its $N$ equally likely possible values without constraint.

We developed some general results for $R$ for some simple geometries including the reorientation of $r$ on a regular polygon and the reorientation of $r$ on a right circular cone. Simple closed-form expressions for $R$ were presented and one interesting result was that the geometric parts of $R$ are independent of $N$. The important problem concerning the manner in which the hopping probabilities (or, equivalently, the correlation times for the hopping process) might depend on $N$ is not addressed here.

We then developed a procedure for determining $R$ resulting from the interaction between a mobile spin free to hop among $N$ sites on a regular polygon and a fixed spin positioned any-

where with respect to the polygon. The algebraic results are too complicated to express in closed form but are contained in computer memory using the computer algebra package *Mathematica*. The results were presented graphically. This geometry is appropriate for the interaction between a methyl group proton and a non-methyl group proton. Several examples of such interactions were discussed and presented. The interaction between each of the three methyl protons and an adjacent peri proton is very strong when the methyl group is oriented with one proton in the plane of the ring next to the peri proton. This new quantitative result can be used with available experimental data to rule that geometry out, in agreement with other spectroscopies and ab initio calculations. The interaction between each of the three methyl protons and an adjacent ortho proton like in methylbenzene is less important, but not negligible. With all these ideas a procedure was presented which allows for the calculation of $R$ in a variety of methyl-substituted molecules and related kinds of systems.

## References

[1] P.A. Beckmann, Phys. Rep. 171 (1988) 85.
[2] A. Abragam, The Principles of Nuclear Magnetism (Oxford University Press, 1961).
[3] C.P. Slichter, Principles of Nuclear Magnetism (Springer-Verlag, Berlin, 1978).
[4] E.O. Stejskal and H.S. Gutowsky, J. Chem. Phys. 28 (1958) 388. In this beautiful and classic paper, the expression for $R$ for a $CH_3$ group is in error by a factor of two.
[5] P.A. Beckmann, Molec. Phys. 41 (1980) 1227.
[6] U. Fano and G. Racah, Irreducible Tensor Sets (Academic Press, New York, 1959) ch. V and Appendix J.
[7] P. Yi, I. Ozier and C.H. Anderson, Phys. Rev. 165 (1968) 92.
[8] M.E. Rose, Elementary Theory of Angular Momentum (Wiley, New York, 1957).
[9] P.A. Beckmann, Molec. Phys. 34 (1977) 665.
[10] D.E. Woessner, J. Chem. Phys. 36 (1962) 1.
[11] P.S. Hubbard, Phys. Rev. 109 (1958) 1153; 111 (1958) 1746.
[12] L.K. Runnels, Phys. Rev. A 134 (1964) 28.
[13] R.L. Hilt and P.S. Hubbard, Phys. Rev. A 134 (1964) 392.

[14] P.S. Hubbard, Phys. Rev. 128 (1962) 650.

[15] P.A. Beckmann, M. Bloom and I. Ozier, Canad. J. Phys. 54 (1976) 1712.

[16] M. Mehring and H.J. Raber, Chem. Phys. 59 (1973) 1116.

[17] A. Kumar and C.S. Johnson Jr., J. Chem. Phys. 60 (1974) 137.

[18] J.D. Cutnell and W. Venable, J. Chem. Phys. 60 (1974) 3795.

[19] P.A. Beckmann, L. Happersett, A.V. Herzog and W.M. Tong, J. Chem. Phys. 95 (1991) 828.

[20] F. Reif, Fundamentals of Statistical and Thermal Physics, (McGraw-Hill, New York, 1965).

[21] N.G. Van Kampen, Stochastic Processes in Physics and Chemistry (North-Holland, Amsterdam, 1981).

[22] P.A. Beckmann, J.W. Emsley, G.R. Luckhurst and D.L. Turner, Molec. Phys. 50 (1983) 699.

[23] P.A. Beckmann, J.W. Emsley, G.R. Luckhurst and D.L. Turner, Molec. Phys. 59 (1986) 97.

[24] H. Wachtel, H. Port and H.C. Wolf, Chem. Phys. Lett. 135 (1987) 506.

[25] P.A. Beckmann, in: Physics and Chemistry of Finite Systems: From Clusters to Crystals, eds. P. Jena, S.N. Khanna and B.K. Rao (Kluwer Academic Publishers, Dordrecht, 1992) p. 357.

[26] C. Palmer, PhD dissertation, Bryn Mawr College (1991), University Microfilms International (Ann Arbor, Michigan, USA; manuscript #9128586).

[27] B.H. Meier, F. Graf and R.R. Ernst, J. Chem. Phys. 76 (1982) 767.

[28] E.R. Andrew and L. Latanowicz, J. Magn. Reson. 68 (1986) 232.

[29] K.G. Conn, P.A. Beckmann, C.W. Mallory and F.B. Mallory, J. Chem. Phys. 87 (1987) 20.

[30] P.A. Beckmann, R.M. Hathorn and F.B. Mallory, Molec. Phys. 69 (1990) 411.

[31] S.A. Streitwieser Jr. and C.H. Heathcock, Introduction to Organic Chemistry (MacMillan, New York, 1981).

[32] S.N. Ege, Organic Chemistry (DC Heath, Lexington, MA, 1984).

[33] S. Clough, Physica B 136 (1986) 145.

[34] J.U. Von Schütz and H.C. Wolf, Z. Naturforsch. A 27 (1972) 42.

[35] F. Imashiro, K. Takegoshi, S. Okazawa, J. Furukawa, T. Terao and A. Saika, J. Chem. Phys. 78 (1983) 1104.

[36] F. Imashiro, K. Takegoshi, K. Hirayama, T. Tereo and A. Saika, J. Org. Chem. 52 (1987) 1401.

[37] F.B. Mallory, C.W. Mallory, K.G. Conn and P.A. Beckmann, J. Phys. Chem. Solids 51 (1990) 129.

[38] K.H. Ladner, D.K. Dalling and D.M. Grant, J. Phys. Chem. 80 (1976) 1783.

[39] P. George, C.W. Bock, J.J. Stezowski, T. Hildenbrand and J.P. Gluster, J. Phys. Chem. 92 (1988) 5656.

[40] X.-Q. Tan, W.A. Majewsk, D.F. Plusquellic and D.W. Pratt, J. Chem. Phys. 94 (1991) 7721.